

Chapter 6. Optical implementation of the three dimensional Fourier transform and correlation

Although three dimensional Fourier transform and correlation of color images have been shown to be useful operations in color image processing, it is not possible to implement them directly in an optical correlator that, at most, processes two dimensional signals. To overcome this problem, an encoding of the three dimensional functions onto two dimensional functions is proposed in this chapter. The proposed encoding defines two dimensional functions in a way that their Fourier spectra, and correlation, encode the three dimensional spectra and three dimensional correlation of the three dimensional signals.

6.1. Two dimensional encoding of three dimensional functions

The three dimensional Fourier transform deals with the color distribution of an image in the same way it does with its spatial distribution. Therefore, each one of the different channels of the image contributes to all the channels of the three dimensional spectrum. As the channels of the image are placed at different positions on the color axis, they contribute to the three dimensional spectrum of the color image with different phase, as the translation theorem indicates (See Section 4.7.2). This phase difference between channels can also be generated by a spatial encoding of the color distribution.

The encoding we propose consists in splitting each pixel of a color image of N channels, onto N consecutive pixels aligned along the x -axis of the image. We illustrate it in Figure 6.1: We have considered a 2×2 pixel image with three color channels, which correspond to the *RGB* components of the color of the image (Figure 6.1a). This color image can be described by the three dimensional function represented in Figure 6.1b. We have represented the encoding of this three dimensional function in Figure 6.1c. It is a two dimensional function in which each 3 pixels on the x -axis represent one pixel of the color image (They would be N pixels for a N channels image). Therefore, it is 3 times wider in the x -direction (N times for a N channels image) than a single channel of the three dimensional function. The first pixel of each group of three represents the red component

of the pixel in the color image, the second pixel represents the green component of the same pixel on the color image, and finally the third one represents the blue component. The fourth pixel corresponds to the red component of the following pixel in the color image, and this way successively.

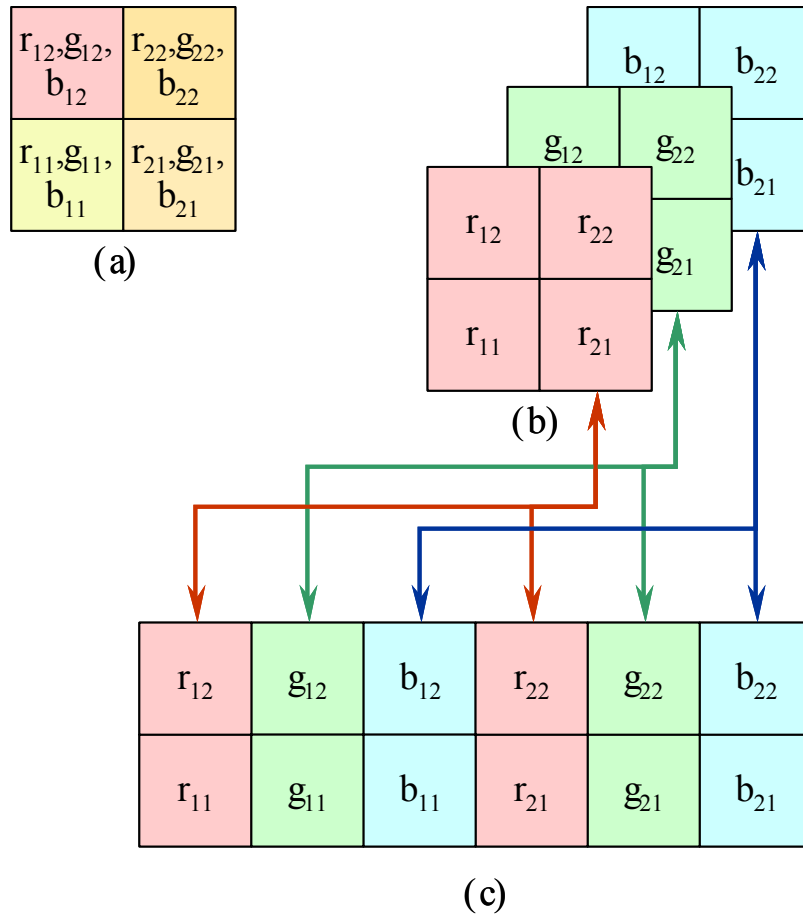


Figure 6.1.(a) Representation of a color image of 2x2 pixels and 3 color channels (RGB). (b) Three dimensional function that describes the color image in a. (c) Two dimensional function that encodes the function in (b).

Let us consider $f_R(\eta_x, \eta_y, \eta_n)$ as a three dimensional function (of three continuous variables) that describes a sampled color image. If $\Delta_x, \Delta_y, \Delta_n$ are the spacing between two consecutive

samples in each direction we can write $f_R(\eta_x, \eta_y, \eta_n)$ in terms of the values $f(x, y, n)$ of the sample as follows:

$$f_R(\eta_x, \eta_y, \eta_n) = \sum_{x=0}^{D_x-1} \sum_{y=0}^{D_y-1} \sum_{n=0}^{N-1} f(x, y, n) \delta(\eta_x - x\Delta_x) \delta(\eta_y - y\Delta_y) \delta(\eta_n - n\Delta_n), \quad (6.1)$$

where $f(x, y, n)$ is the value of the n -th channel at $(\eta_x = x\Delta_x, \eta_y = y\Delta_y)$, that is, the x -th column and y -th row of the sampled image. The size of the image in pixels is $D_x \times D_y$ and N indicates the number of channels that the image has. The image is completely determined by $f(x, y, n)$, which is a function of three integer variables.

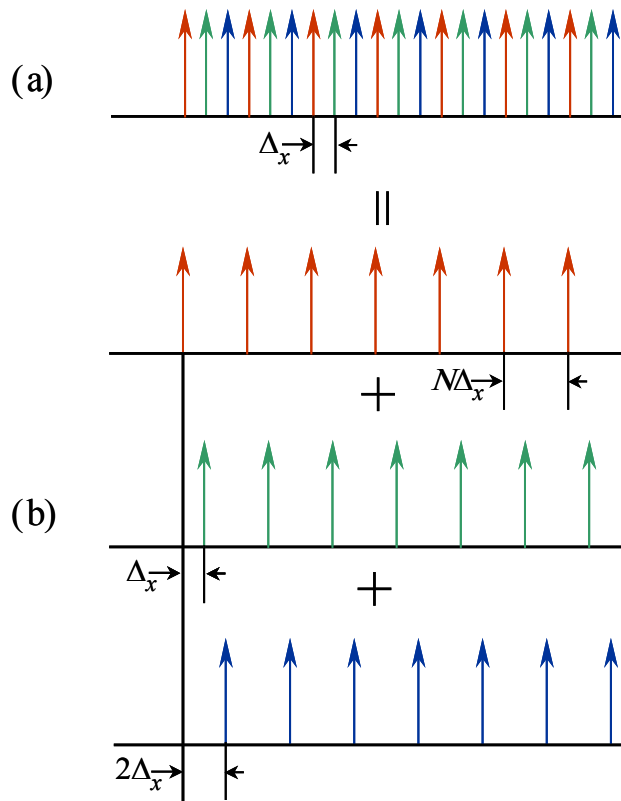


Figure 6.2. Scheme of the sampling along the x-axis for the encoding technique. (a) Sampling for the encoding function. (b) Decomposition of the sampling for the encoding image as the addition of the sampling for each channel of the encoded function.

The proposed encoding technique consists of generating a discrete function $g_R(\eta_x, \eta_y)$, which will be referred to as the *encoding function*, with the values of $f(x, y, n)$, the *encoded function*. The encoding function is generated by placing along the x-axis the values for all the color components of one pixel before placing the components for the next pixel. We have illustrated it in Figure 6.2a. We observe that this sampling function can be conceived as the addition of the samplings for each channel. For each channel, the spacing between two consecutive pixels is N times the sampling spacing Δ_x (Figure

6.2b). In addition, the sampling for the n -th channel is shifted by $n\Delta_x$ from the origin.

The above described addition of the samples for each channel leads to the following expression of $g_R(\eta_x, \eta_y)$:

$$g_R(\eta_x, \eta_y) = \sum_{n=0}^{N-1} \sum_{x=0}^{D_x-1} \sum_{y=0}^{D_y-1} f(x, y, n) \delta(\eta_x - [Nx + n]\Delta_x) \delta(\eta_y - y\Delta_y), \quad (6.2)$$

As $g_R(\eta_x, \eta_y)$ is also a discrete function we can write it in terms of a function $g(x, y)$ of two integer variables that take values in the range $x \in [0, ND_x-1]$ and $y \in [0, D_y-1]$:

$$g_R(\eta_x, \eta_y) = \sum_{x=0}^{ND_x-1} \sum_{y=0}^{D_y-1} g(x, y) \delta(\eta_x - x\Delta_x) \delta(\eta_y - y\Delta_y). \quad (6.3)$$

$g(x, y)$ can be written as a function of $f(x, y, n)$ as follows,

$$g(x, y) = \sum_{n=0}^{N-1} \sum_{x'=0}^{D_x-1} f(x', y, n) \delta_K(x - Nx' - n). \quad (6.4)$$

That is, $g(x, y)$ comes from the addition (sum over n) of the samples of the N channels of $f(x, y, n)$ (sum over x').

It is easy to show that, by using the expression in eq.4 we can write the explicit dependence of $g_R(\eta_x, \eta_y)$ on $f(x, y, n)$. This is done next.

$$g_R(\eta_x, \eta_y) = \sum_{x=0}^{ND_x-1} \sum_{y=0}^{D_y-1} \left[\sum_{n=0}^{N-1} \sum_{x'=0}^{D_x-1} f(x', y, n) \delta_K(x - Nx' - n) \right] \times \delta(\eta_x - x\Delta_x) \delta(\eta_y - y\Delta_y). \quad (6.5)$$

As the indices on the series are independent, and by the properties of δ_K we can simplify x ,

$$g_R(\eta_x, \eta_y) = \sum_{j=0}^{D_y-1} \sum_{n=0}^{N-1} \sum_{x'=0}^{D_x-1} f(x', y, n) \delta(\eta_x - [Nx' + n]\Delta_x) \delta(\eta_y - y\Delta_y). \quad (6.6)$$

Which is the same expression as in eq.2, as we wanted to demonstrate.

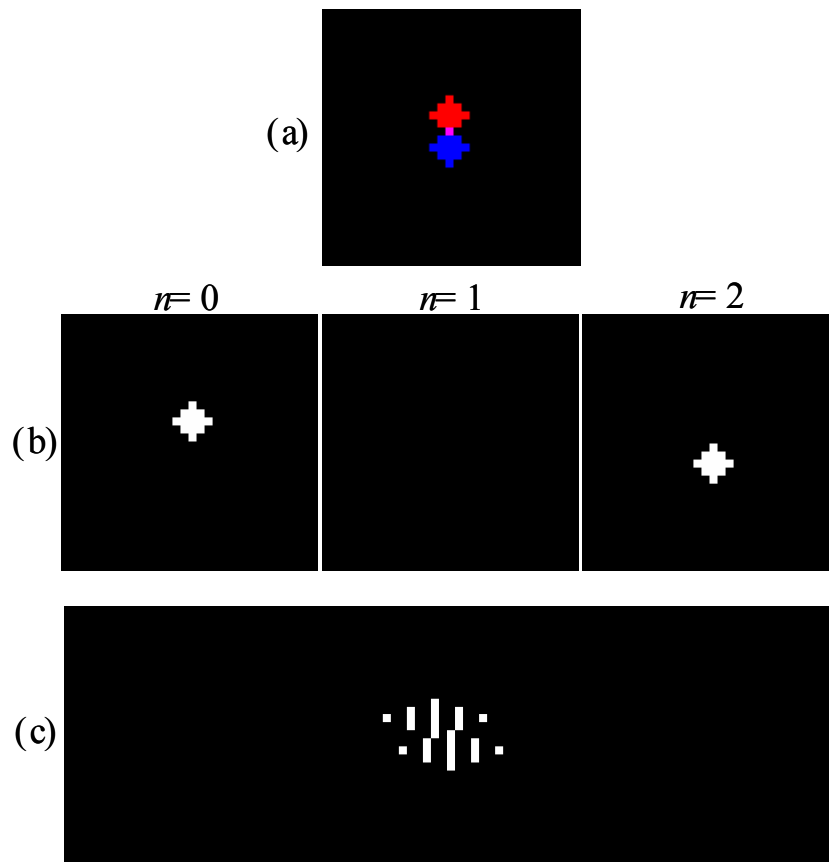


Figure 6.3. Example of encoding of the three dimensional function that describes a color image. (a) Original color image. (b) RGB channels. (c) Encoding function. The scale of all the images has been magnified to make the pixels visible.

An example of the encoding of a three dimensional function is given in Figure 6.3. The color image that we consider is

represented in Figure 6.3a. It consists of two shapes (two squares of 5-pixels diagonal) in blue and red, at different positions, that partially overlap. The common pixel is in magenta, that results from the addition of red and blue. The channels of the three dimensional function (the *RGB* channels of the color image) are displayed in Figure 6.3b. The black and white image resulting from the encoding is represented in Figure 6.3c. It has been magnified so as to make visible the pixels. Each pixel of the color image has been encoded into three pixels. The first of each three of them corresponds to the $n=0$ channel (red), the second to the $n=1$ channel (green) and the third to the $n=2$ channel (blue).

6.2.Encoding of the 3D Fourier transform

As the frequency spectra of $f_R(\eta_x, \eta_y, \eta_n)$ and $g_R(\eta_x, \eta_y)$ are determined by the discrete Fourier transform of $f(x, y, n)$ and $g(x, y)$, except by a scale factor, determined by the sampling frequency, we will deal with the functions of discrete variable. So, we will consider the spectrum of $f(x, y, n)$, denoted as $F(u, v, m)$, which is given by the three dimensional Fourier transform as follows:

$$F(u, v, m) = \frac{1}{D_x D_y N} \sum_{x=0}^{D_x-1} \sum_{y=0}^{D_y-1} \sum_{n=0}^{N-1} f(x, y, n) \exp \left[-i2\pi \left(\frac{ux}{D_x} + \frac{vy}{D_y} + \frac{mn}{N} \right) \right]. \quad (6.7)$$

As the N pixels in the encoding function that correspond to the same pixel of the color image are shifted each other, they

contribute with a different phase to the spectrum of $g(x,y)$, noted as $G(u,v)$, that is given by

$$G(u,v) = \frac{1}{D_x D_y N} \sum_{x=0}^{ND_x-1} \sum_{y=0}^{D_y-1} g(x,y) \exp \left[-i2\pi \left(\frac{ux}{ND_x} + \frac{vy}{D_y} \right) \right]. \quad (6.8)$$

To show the way in which $G(u,v)$ encodes $F(u,v,m)$ we write the explicit dependence of $g(x,y)$ on $f(x,y,n)$, then we get

$$G(u,v) = \frac{1}{D_x D_y N} \sum_{x=0}^{ND_x-1} \sum_{y=0}^{D_y-1} \left[\sum_{x'=0}^{D_x-1} \sum_{n=0}^{N-1} f(x',y,n) \delta_K(x - Nx' - n) \right] \times \exp \left[-i2\pi \left(\frac{ux}{ND_x} + \frac{vy}{D_y} \right) \right]. \quad (6.9)$$

As the series indices are independent each other, they can be swapped each other and the Kronecker's delta function can be simplified. So, we obtain

$$G(u,v) = \frac{1}{D_x D_y N} \sum_{x'=0}^{D_x-1} \sum_{y=0}^{D_y-1} \sum_{n=0}^{N-1} f(x',y,n) \exp \left[-i2\pi \left(\frac{ux'}{D_x} + \frac{vy}{D_y} + \frac{un}{ND_x} \right) \right]. \quad (6.10)$$

By comparing eqs. 7 and 10 it follows that $G(u,v)$ can be written as an encoding of the three dimensional spectrum of $f(x,y,n)$

$$G(u,v) = F \left(u, v, \frac{u}{D_x} \right). \quad (6.11)$$

Of course, while $F(u,v,m)$ is a function of three variables, $G(u,v)$ is function of only two variables. Then, one degree of freedom is lost. Note, in eq.11 that the variable corresponding to the color component of the frequency in F depends linearly on the x -

component of the frequency (u). To illustrate this, we have represented in Figure 6.4 the dependence between the linked variables. The y -component of the frequency is not involved in the encoding and therefore it is not represented.

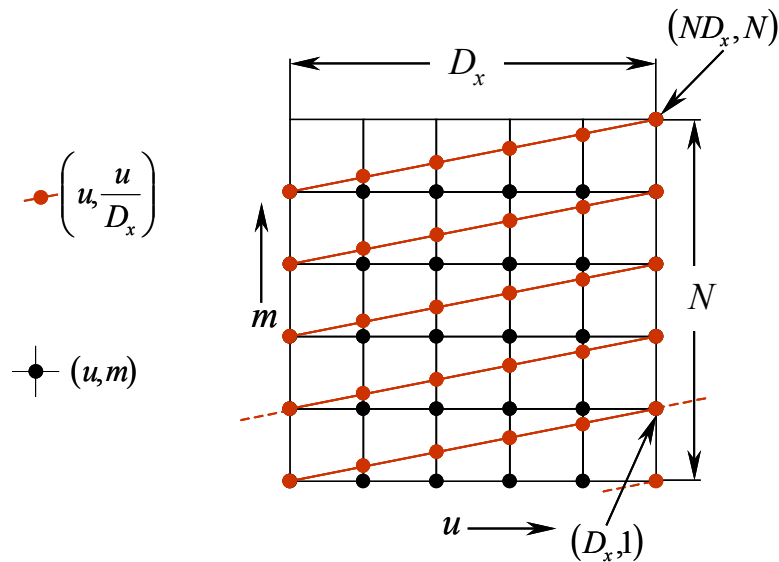


Figure 6.4. Representation of the sampling for the spectrum of the encoding function (red dots) and the spectrum of the encoded function (black dots).

The grid of black dots (Figure 6.4) represents the points where the three dimensional spectrum $F(u, v, m)$ is sampled when the discrete three dimensional Fourier transform of $f(x, y, n)$ is performed. In this case u and m are independent variables and they can be represented in a cartesian frame. The line of red dots in Figure 6.4 represents the points where the spectrum $F(u, v, m)$ is sampled when it is encoded on $G(u, v)$. We have taken into account that there is a linear dependence (eq.11) between u and m in such a way that when $u=D_x$ then $m=1$. We have also taken into account that $F(u, v, m)$ is a periodic function, so we have represented the values where $u>D_x$. by

their replicas in the first period. As in $G(u,v)$ u takes values between 0 and ND_x , there are N lines that sample the N channels of the period. We can write $u=u'+mD_x$. This way, m indexes the period and u' indexes the position in the x -direction, relative to the m -th period. Then, we can write $G(u,v)$ as follows

$$G(u'+mD_x, v) = F\left(u'+mD_x, v, m + \frac{u'}{D_x}\right). \quad (6.12)$$

Because F has period D_x along the x -axis, we can consider the replicas in the first period (See Figure 6.4). Then we can write

$$G(u'+mD_x, v) = F\left(u', v, m + \frac{u'}{D_x}\right). \quad (6.13)$$

So m , that takes values between 0 and $N-1$, represents the m -th channel of the spectrum, and the remaining fractional term represents the deviation from the true sampling, which is always less than one (less than the sampling spacing).

6.3. shifted carrier encoding

The encoding proposed in the previous sections can also be described in terms of a multiplexing of the samples for the different channels by means of carrier functions. This approach allows us to study the relation of the encoding with the sampling of the physical signal, and to propose an alternative sampling of the three dimensional signal so as to obtain the exact values of its three dimensional spectrum.

Let us consider the two dimensional encoding function $g(x,y)$ as the addition of the N channels of the three dimensional signal $f(x,y,n)$ (see Figure 6.5a). Each channel is multiplied by a discrete comb function, defined as

$$\text{comb}_N(x) \equiv \sum_{x'=-\infty}^{+\infty} \delta_K(x - Nx'), \quad (6.14)$$

which is called the *carrier* of that channel. Because the period in pixels of the carrier functions is equal to the number of channels of the three dimensional signal, N , and the carrier of the n -th channel is shifted n pixels with respect to the origin, the encoding function can be written as

$$g(x, y) = \sum_{n=0}^{N-1} f_{DI}(x, y, n) \text{comb}_N(x - n). \quad (6.15)$$

Here $f_{DI}(x,y,n)$ is a function that results from dilatation of the sample of the n -th channel by a factor N along the x direction. The dilated function is the discrete function that comes from inserting $N-1$ pixels that value zero between two pixels of $f(x,y,n)$, consecutive along the x direction. $f_{DI}(x,y,n)$ takes the value $f(x',y,n)$ in the points (Nx',y,n) , and the value zero elsewhere. Note that the comb function in equation 15 is shifted by a n/N of the sample spacing of the dilated function. Therefore the product is zero, because the nonzero points do not coincide. This can be avoided by means of an interpolation of the dilated function. The most simple interpolation technique consists of considering the value of the previous neighbor pixel.

This is equivalent to shift the dilated function by n pixels, in the same way as in Section 6.1. Therefore $f_{DI}(x,y,n)$ can be written

$$f_{DI}(x,y,n) = \sum_{x'=0}^{ND_x-1} f(x',y,n)\delta(x - Nx' - n). \quad (6.16)$$

This way, the spectrum of the encoding function, $G(u,v)$ can be written as the addition of the convolutions of the two dimensional spectra of each channel and the spectrum of its carrier function. Because the carriers for the different channels are comb functions with different shifts, their spectra are a comb function with different linear phases, as follows:

$$G(u,v) = \sum_{n=0}^{N-1} F_{DI}^{2D}(u,v,n) * \text{comb}_{D_x}(u) \exp\left(-i \frac{2\pi}{ND_x} nu\right). \quad (6.17)$$

Here $F_{DI}^{2D}(u,v,n)$ is the two dimensional spectrum of the n -th channel of $f_{DI}(x,y,n)$, which is a dilatation by a factor $1/N$ of the spectrum of $f(x,y,n)$. If we develop the explicit expression of the comb function we obtain:

$$G(u,v) = \sum_{n=0}^{N-1} F_{DI}^{2D}(u,v,n) * \sum_{u_1=-\infty}^{+\infty} \delta_K(u - u_1 D_x) \exp\left(-i \frac{2\pi}{ND_x} nu\right). \quad (6.18)$$

And by expanding the expression for the convolution we get

$$G(u,v) = \sum_{u_2=-\infty}^{+\infty} \sum_{u_1=-\infty}^{+\infty} \sum_{n=0}^{N-1} F_{DI}^{2D}(u - u_2, v, n) \exp\left(-i \frac{2\pi}{ND_x} nu_2\right) \delta_K(u_2 - u_1 D_x). \quad (6.19)$$

By applying the properties of the Kronecker's delta function we can simplify the expression

$$G(u,v) = \sum_{u_1=-\infty}^{+\infty} \sum_{n=0}^{N-1} F_{DI}^{2D}(u-u_1D_x, v, n) \exp\left(-i\frac{2\pi}{N}nu_1\right). \quad (6.20)$$

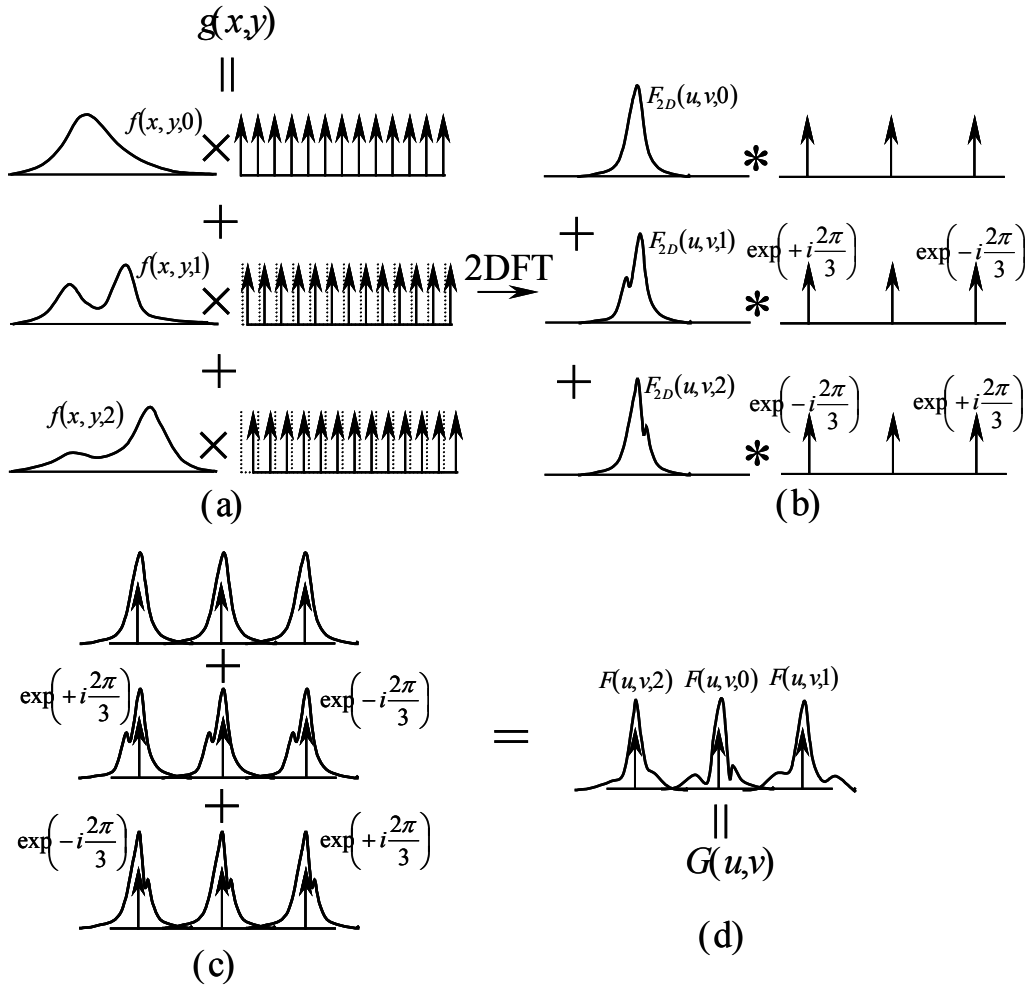


Figure 6.5. Interpretation of the encoding of the three dimensional Fourier transform. (a) The color channels are multiplied by shifted comb functions. (b) Convolution of the spectra for the channels and for the comb distribution. (c) result of the convolution. (d). The different channels of the three dimensional spectrum.

The series on the index n can be written as a translation of the three dimensional Fourier transform of $f(x,y,n)$.

$$G(u,v) = \sum_{u_1=-\infty}^{+\infty} F(u-u_1D_x, v, u_1). \quad (6.21)$$

Because the range of the variable u is ND_x , the index u_1 takes values between zero and $N-1$. And it indicates the channel of the three dimensional spectrum of $f(x,y,n)$

Figure 6.5 illustrates the interpretation in terms of carrier functions of the encoding technique. In Figure 6.5a the encoding function $g(x,y)$ is represented as the addition of the channels multiplied by their carrier functions, which are comb functions shifted each other. The two dimensional spectrum $G(u,v)$ of the encoding function is represented in Figure 6.5b as the addition of the convolutions of the two dimensional spectra of the channels with the spectra of their carriers. The period of the carriers is N pixels, so their discrete spectra present N deltas functions in one period of $G(u,v)$. In addition, as the carriers are shifted each other, their spectra have different linear phase factors. The phase difference between two consecutive deltas of the spectrum for the n -th carrier is $2\pi n/N$ because it is shifted n/N of its period. The convolution of the spectra of the channels with the N deltas corresponding to the comb function produces N replicas of the two dimensional spectra of the channels (Figure 6.5c). Nevertheless, as the deltas have different phase, the replicas are multiplied by a different phase factor, determined by the linear phase introduced by the shift of the carriers. Therefore, considering the contributions of the N carriers, for each one of the N deltas of their spectra, the addition of the two dimensional spectra of the N channels, multiplied by a phase factor is obtained. The phase factor of

each channel is the same as the phase factor produced by its shift along the color axis. Therefore, the N channels of the three dimensional spectrum of the encoded function $f(x,y,n)$ are obtained in the N periods of the spectrum of the carrier functions (Figure 6.5d).

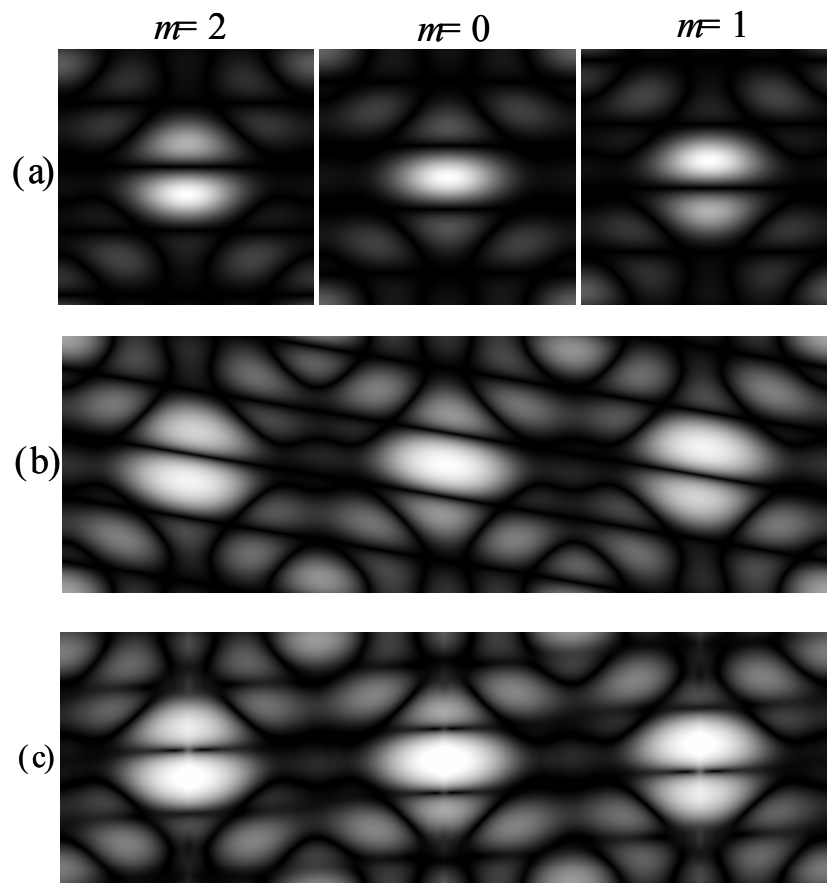


Figure 6.6. Example of encoding of the three dimensional Fourier transform. (a) Magnitude of the channels of the spectrum obtained by three dimensional Fourier transform. (b) Magnitude of the spectrum of the encoding function. (c) Magnitude of the spectrum of the encoding function for a resample by sinc interpolation of the three dimensional signal.

In this case, the encoding of the three dimensional spectrum of $f_{DI}(x,y,n)$ is exact, however, if $f_{DI}(x,y,n)$ is obtained from a discrete function like $f(x,y,n)$ an interpolation operation has to

be performed. Depending on the interpolation technique a deviation is introduced between the spectrum obtained by performing the three dimensional Fourier transform and the spectrum obtained by performing the two dimensional Fourier transform of the encoding function.

An example of the encoding of the three dimensional spectrum of a color image is given in Figure 6.6. We have considered the image in Figure 6.3.

The three channels of the 3D spectrum of the color image, digitally obtained, are presented in Figure 6.6a. As the original scene could be considered as the convolution of one square, with two Kronecker deltas, located at two different positions and channels, the spectrum will be the interference pattern of these deltas, that is a cosine function whose argument depends on the spatial variables and on the channels index, multiplied by the Fourier transform of the square, that is, a $\text{sinc}(x+y)\text{sinc}(x-y)$ function. Figure 6.6b shows the two dimensional spectrum of the encoded image, which is 3 times wider than a single channel of the three dimensional spectrum of the color image. The three channels of the 3D spectrum can be identified there. They are similar to the three channels of the three dimensional spectrum of the original color image. However, a difference in the nodes of the interference patterns can be observed. In the case of the spectrum obtained by three dimensional Fourier transform the nodes are horizontal, and located at different positions. On the other hand, for the

spectrum obtained from the encoded image the nodes are not horizontal. This is due to the coordinate shift introduced by the previous neighbor interpolation method. Figure 6.6c represents the two dimensional spectrum of the encoding function, but in that case we have resampled the channels by means of sinc interpolation. In this case the nodes of the interference pattern in the different areas of the two dimensional spectrum are horizontal, like in the three dimensional spectrum digitally obtained.

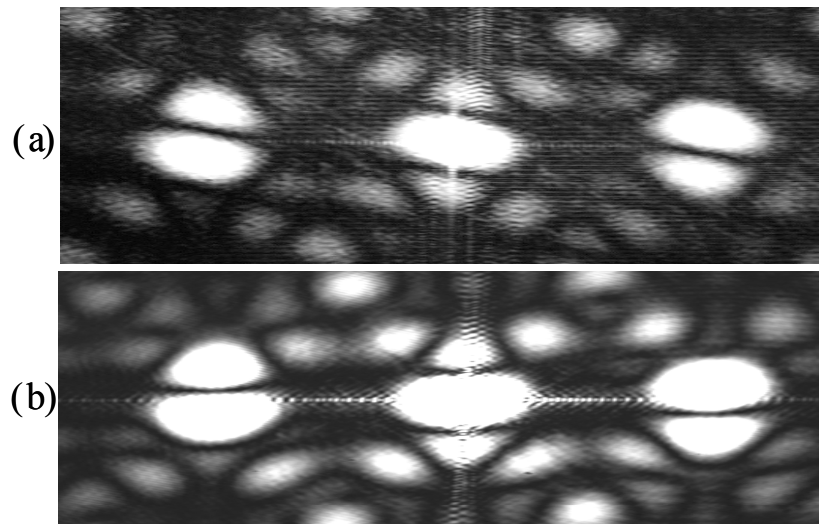


Figure 6.7. (a) Diffraction pattern of the encoding image. (b) Diffraction pattern of the encoding function for a resampling by sinc-interpolation of the three dimensional function.

We have represented in Figure 6.7 the optically obtained channels of the three dimensional spectrum for the color image in Figure 6.6. To obtain them, the three dimensional function has been encoded onto a two dimensional function following the described technique. Then, the obtained two dimensional function has been used as the input image of a Fraunhofer

diffractometer. Figure 6.7a represents the intensity of the Fraunhofer diffraction pattern for the encoding image. There, the nodes of the interference pattern between the squares in the different channels are not horizontal because the three dimensional function has not been resampled, what is equivalent to consider the previous neighbor interpolation in the resampling. The diffraction pattern in Figure 6.7b has been obtained by using as the input scene for the diffractometer the encoding function for three dimensional function that has been resampled by sinc interpolation

6.4.Color encoding vs Spatial encoding

The above exposed study shows how to reduce one dimension of the treated signal by encoding the information along one of the variables onto another variable. We have considered the encoding of the color variable onto one of the spatial variables, by splitting each pixel of the encoded function, determined by the value of the x -variable, in N pixels of the encoding function. Nevertheless, it is also possible to encode the x -variable onto the color variable. That is, to split each channel, determined by the value of the color variable, in D_x channels. We refer to these two strategies as color encoding, when the color dimension is reduced, and spatial encoding, when the reduced dimension is one of the spatial ones.

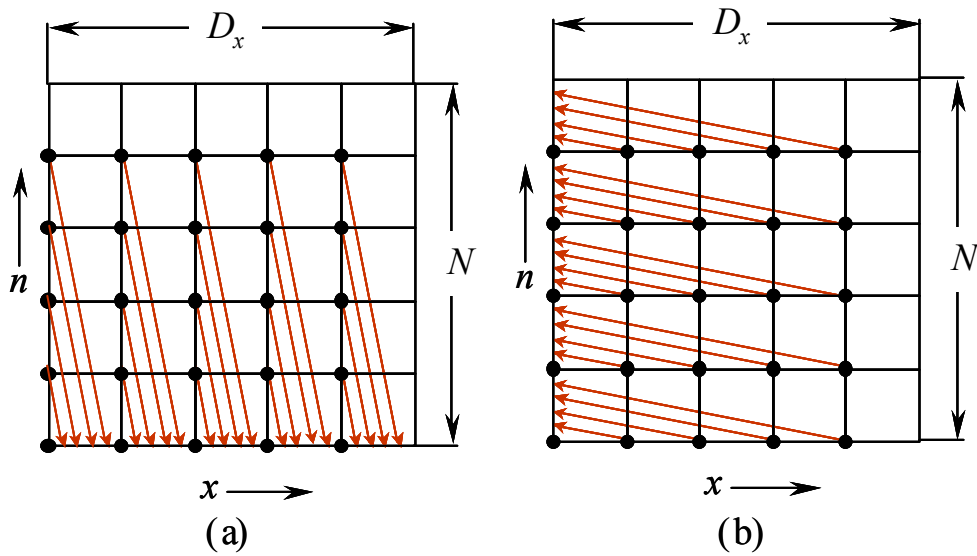


Figure 6.8.(a) encoding of the color information onto the spatial axis. (b) encoding of the spatial information onto the color axis.

Figure 6.8 shows an scheme of these two encoding approaches. We have considered only one spatial variable (x) and the color variable (n). In Figure 6.8a The color information is encoded onto the x -variable, that is, the values of all the channels of one pixel are represented together along the color axis, and so on with the next pixels. The other approach is represented in Figure 6.8.b. There the x -variable is encoded onto the color axis. That is, all the pixels of one channel are represented and after that all the pixels for the following channel are represented. Therefore, what is obtained is the juxtaposition of the channels of the color image.

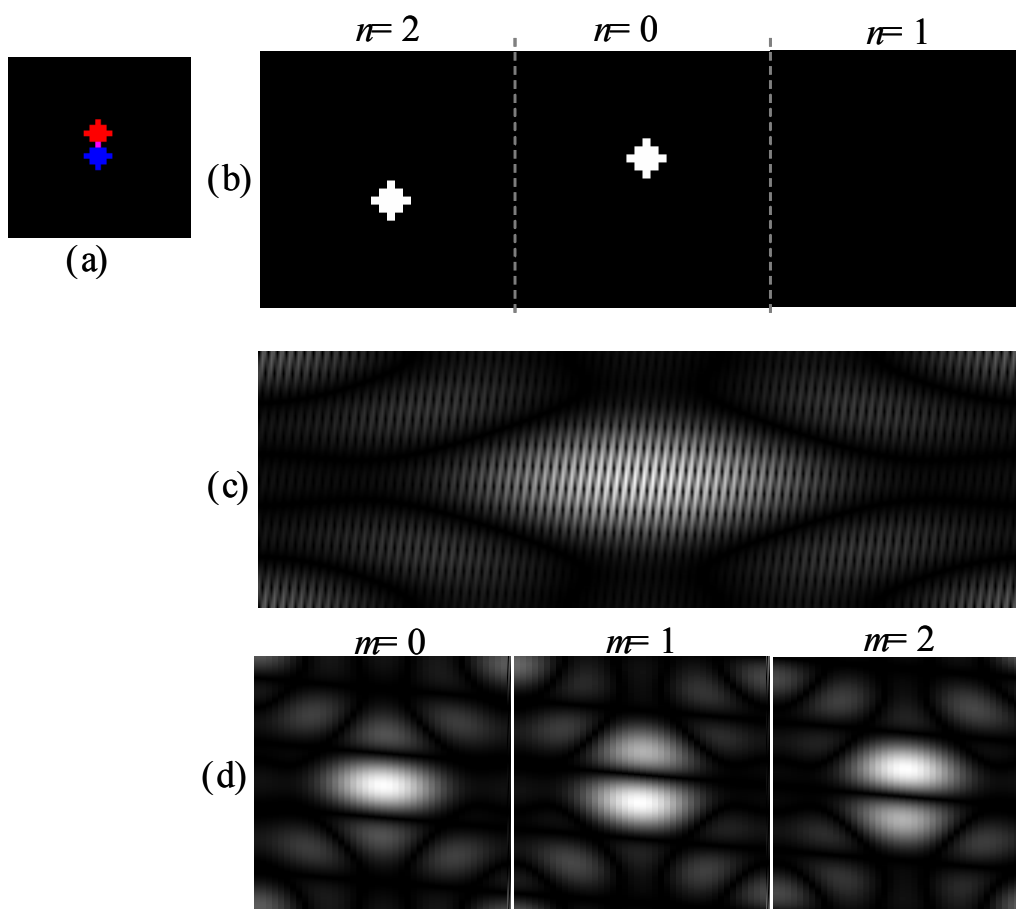


Figure 6.9.(a) Target color image, it has been zoomed to make the shapes visible (b) Two dimensional image resulting from the encoding. (c) Spectrum of the encoding function. (d) Decoded channels of the spectrum of the encoding function.

Figure 6.9 represents the encoding of the spatial variable onto the color axis. The color image in Figure 6.9a is encoded following this approach, so, the encoding function is the juxtaposition of the channels (Figure 6.9b). When the two dimensional Fourier transform is performed, the spectrum represented in Figure 6.9c is obtained. There, the three channels of the three dimensional spectrum are encoded. In this case there are D_x periods of N pixels, being each period corresponding to a value of the u -variable. Once this two

dimensional spectrum is decoded, the channels of the three dimensional spectrum of the image are obtained (Figure 6.9d)

6.5.Properties of the encoded Fourier transform

The proposed technique to encode three dimensional functions preserves the properties of the three dimensional Fourier transform shown in Chapter 5. In this section we give the interpretation in the encoded spectrum for some of them.

6.5.1. *Spectrum of a black and white image*

Let us consider a black and white image, that is, an image in which all the channels are identical. In this case, the three dimensional function that describes the image does not change along the color axis, in other words, the color distribution of any pixel is a constant. That means that, for black and white images, the three dimensional spectrum is zero for any frequency with a nonzero color component. That is, the only nonzero channel of the three dimensional spectrum of a black and white image is the central channel ($m=0$).

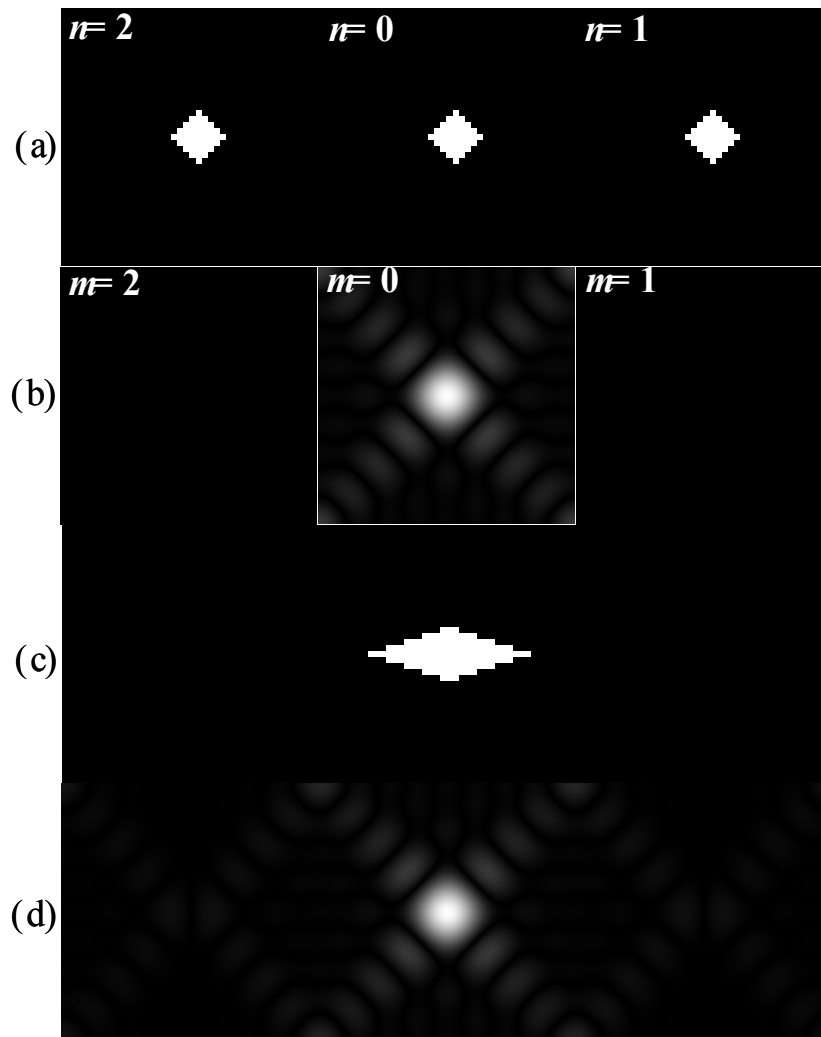


Figure 6.10. Example of three dimensional encoding of a black and white image. (a) Amplified view of the channels of the original image. (b) Digitally obtained three dimensional spectrum. (c) Amplified view of the encoding image. (d) Two dimensional spectrum of the encoding image.

This property is preserved by the exposed encoding technique. Let us consider the three dimensional function that describes a black and white image. In this case all the channels are identical, as Figure 6.10a shows. As predicted, the three dimensional spectrum (Figure 6.10b) is null out of the $m=0$ channel. When the three dimensional function is encoded onto a two dimensional function, every pixel is spread to N pixels

with the same value, because all the channels are identical. So, the encoding image is equal to the original but N times wider. We can say that a dilatation by a factor N along the x -direction is applied, as Figure 6.10c shows. This way, by the dilatation theorem, we find that the spectrum of the encoding image is dilated by a factor $1/N$. That means that it just covers the D_x central pixels, which correspond to the $m=0$ channel of the three dimensional spectrum of the encoded color image, what is shown in Figure 6.10d.

6.5.2. ***Spectrum of a monochromatic image***

The reciprocal situation to a black and white image is to consider a monochromatic image, in which all the channels except one are null. In this case the three dimensional spectrum is constant along the color-frequency axis. This property is also preserved by the encoding technique.

Let us consider a monochromatic image, that is, an image with only one channel different from zero. In this case the color distribution of any pixel is a delta distribution. Therefore, the three dimensional spectrum is constant along the color axis, or in other words, the N channels of the three dimensional spectrum are identical.

We have illustrated it in Figure 6.11. We have considered a monochromatic image (Figure 6.11a) and calculated its three dimensional Fourier transform. The channels of its three dimensional spectrum are represented in Figure 6.11b. As

predicted the three channels are identical each other. For this monochromatic image, the encoded function consists of the nonzero channel, dilated by a factor N and multiplied by a comb function of period N , as can be observed in Figure 6.11c. Therefore, applying the convolution theorem for two dimensional functions, we find that the spectrum of the encoding function is the convolution of the two dimensional spectrum of the nonzero channel, dilated by a factor $1/N$ with a comb function of period D_x . So, N identical replicas of the spectrum of this channel are obtained, as observed in Figure 6.11d.

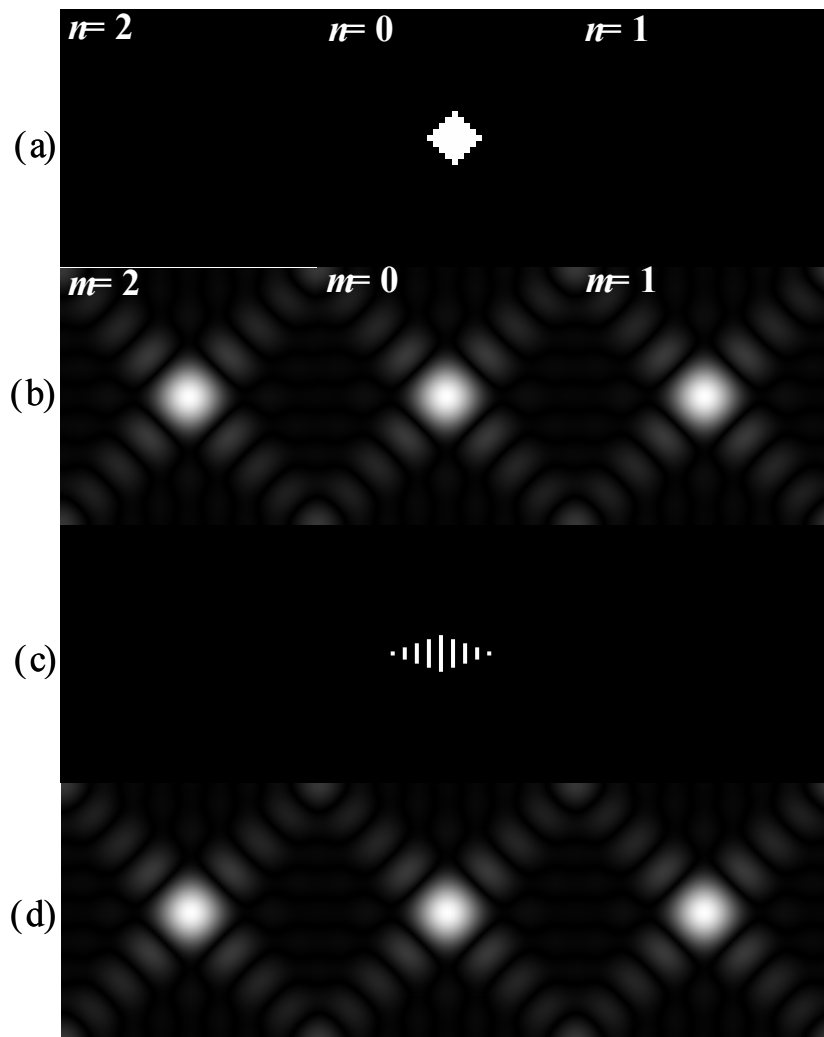


Figure 6.11. Encoding of the spectrum of a monochromatic image. (a) RGB channels of the monochromatic image. (b) channels of the three dimensional spectrum. (c) Encoding image. (d) Spectrum of the encoding image.

6.5.3. *Inversion theorem*

Let us consider that we apply twice the three dimensional direct Fourier transform, we obtain the original image with the three coordinate axes inverted. That means that the color distribution is also inverted and the n -th channel is swapped with the $(N-n)$ th. Let us consider the encoding of the image. In this case the channels are ordered along the x -axis. Therefore, when the x -

axis is inverted by the double direct Fourier transform. Also the order of the channels is inverted.

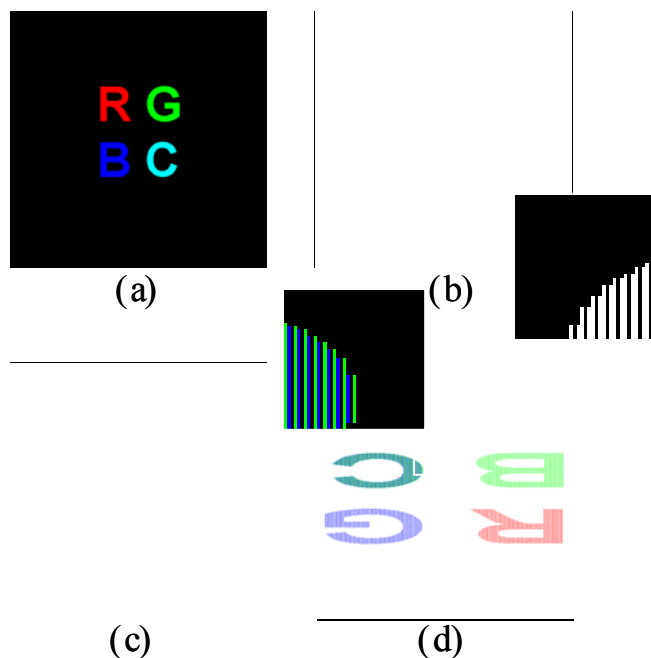


Figure 6.12. Illustration of the encoding of the inversion theorem: (a) Original color image. (b) Corresponding encoding image. (c) Image retrieved after two direct Fourier Transform operations applied to the encoding image. (d) pseudo-coloration of the retrieved image, coloring in red the pixels corresponding to the $n=0$ channel, and in green and blue the pixels corresponding to the $n=1$ and $n=2$ channels.

We illustrate this with an example in Figure 6.12. We have considered a color image with four letters in different colors: a red R, a green G, a blue B and a C in cyan. (Figure 6.12a). The central part of the corresponding encoding image is shown in Figure 6.12b. After the application of two direct Fourier transforms to the two dimensional encoding image we obtain its spatial inversion (Figure 6.12c). Because of this inversion, the pixels that corresponded to the $n=1$ channel, now are located at the positions that correspond to the $n=2$ channel. To show this,

we have painted each pixel in the color of its corresponding channel in Figure 6.12d. There, one can observe that the $n=1$ and $n=2$ channels (green and blue) have been interchanged and therefore the B is now green and the G is blue. The red has not been changed. And because the cyan has the same amount of green and blue it has not changed either.

6.6. Encoding of the three dimensional correlation

The technique proposed to encode color images and to perform the three dimensional Fourier transform is valid to perform the three dimensional correlation of three dimensional Functions as is shown next. We analyze how the three dimensional correlation is encoded by the two-dimensional correlation of the encoding functions. We pay special attention to the $n=0$ channel of the three dimensional correlation because it contains the information useful for color pattern recognition.

Let us consider the three dimensional correlation of two color images, described by the functions $f(x,y,n)$ and $g(x,y,n)$, that are encoded onto the two dimensional functions $f_E(x,y)$ and $g_E(x,y)$. They are given by the following expressions, for the scene,

$$f_E(x,y) = \sum_{n=0}^{N-1} \sum_{x_1=0}^{D_x-1} f(x_1,y,n) \delta_K(x - Nx_1 - n). \quad (6.22a)$$

and for the reference

$$g_E(x,y) = \sum_{n=0}^{N-1} \sum_{x_1=0}^{D_x-1} g(x_1,y,n) \delta_K(x - Nx_1 - n). \quad (22b)$$

The two dimensional correlation of $f_E(x,y)$ and $g_E(x,y)$ is defined as the addition of the products of $f_E(x,y)$ and $g_E^*(x,y)$ for all the possible relative translations. This is expressed as follows

$$C_{2D}[f_E, g_E](x, y) = \sum_{x_1=0}^{ND_x-1} \sum_{y_1=0}^{D_y-1} f_E(x_1, y_1) g_E^*(x_1 - x, y_1 - y). \quad (6.23)$$

For replacing in this expression the encoding functions by the three dimensional functions they encode it is necessary to develop the translation of $g_E^*(x,y)$ in terms of $g(x,y,n)$. Note that the color dimension is encoded onto one spatial dimension, and therefore the spatial translations of $g_E^*(x,y)$ encode both spatial and color translations of $g(x,y,n)$. We consider a translation of $Nx-n$ pixels along the x -axis. It can be written as

$$g_E(x - Nx' - n', y) = \sum_{n_1=0}^{N-1} \sum_{x_1=0}^{D_x-1} g(x_1, y, n_1) \delta_K(x - Nx' - n' - Nx_1 - n_1). \quad (6.24)$$

If we define $x_2 = x' + x_1$ and $n_2 = n' + n_1$ we can simplify the expression:

$$g_E(x - Nx' - n', y) = \sum_{n_2=n'}^{N+n'-1} \sum_{x_2=x'}^{D_x+x'-1} g(x_2 - x', y, n_2 - n') \times \delta_K(x - Nx_2 - n_2). \quad (6.25)$$

When n_2 is bigger than N it is convenient to write it as $n_2 = N + n_3$, where n_3 is smaller than N . This way, the component of the translation along the color axis is given by n_3 . Similarly, when $x_2 > D_x$ it can be written as $x_2 = D_x + x_3$. So, we write the following

four series, that come from splitting the terms where n_2 or x_2 are bigger than $N-1$ or D_x-1 , respectively.

$$\begin{aligned}
 g_E(x - Nx' - n', y) = & \sum_{n_2=n'}^{N-1} \sum_{x_2=x'}^{D_x-1} g(x_2 - x', y, n_2 - n') \delta_K(x - Nx_2 - n_2) \\
 & + \sum_{n_2=n'}^{N-1} \sum_{x_3=0}^{x'-1} g(D_x + x_3 - x', y, n_2 - n') \\
 & \times \delta_K(x - ND_x - Nx_3 - n_2) \\
 & + \sum_{n_3=0}^{n'-1} \sum_{x_2=x'}^{D_x-1} g(x_2 - x', y, N + n_3 - n') \\
 & \times \delta_K[x - N(x_2 + 1) - n_3] \\
 & + \sum_{n_3=0}^{n'-1} \sum_{x_3=0}^{x'-1} g(D_x + x_3 - x', y, N + n_3 - n') \\
 & \times \delta_K[x - N(D_x + x_3 + 1) - n_3]
 \end{aligned} \quad . \quad (6.26)$$

And taking into account that $g(x,y,n)$ has period D_x on x and period N on n , we can simplify it and leave only two terms, as follows

$$\begin{aligned}
 g_E(x - Nx' - n', y) = & \sum_{n_2=n'}^{N-1} \sum_{x_2=0}^{D_x-1} g(x_2 - x', y, n_2 - n') \delta_K(x - Nx_2 - n_2) \\
 & + \sum_{n_3=0}^{n'-1} \sum_{x_2=0}^{D_x-1} g[x_2 - (x'+1), y, n_3 - n'] \delta_K(x - Nx_2 - n_3)
 \end{aligned} \quad . \quad (6.27)$$

The first term in this expression corresponds to a part of the encoding of the three dimensional function, shifted by x' pixels along the x direction and by n' pixels along the color axis (See the green arrows in Figure 6.13). In the second term, however, a mismatch of one pixel along the x direction appears (See the red arrows in Figure 6.13).

By adding and subtracting the missing terms for the first series we obtain

$$g_E(x - Nx' - n', y) = \sum_{n_2=0}^{N-1} \sum_{x_2=0}^{D_x-1} g(x_2 - x', y, n_2 - n') \delta_K(x - Nx_2 - n_2) + E(x', y, n'). \quad (6.28)$$

where $E(x', y, n')$ is the error produced by the translation mismatch. It can be written as follows

$$E(x', y, n') = \sum_{n_2=0}^{n'-1} \sum_{x_2=0}^{D_x-1} (g[x_2 - (x'+1), y, n_2 - n'] - g(x_2 - x', y, n_2 - n')) \times \delta_K(x - Nx_2 - n_2) \quad (6.29)$$

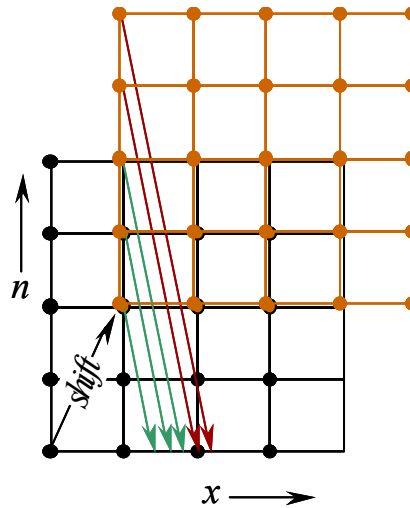


Figure 6.13. Encoding of a shifted function. The green arrows represent the terms for which the encoding is exact. The red arrows represent the terms for which there is a one-pixel mismatch.

Let us remark that $E(x, y, n')$ is zero for $n'=0$. That means that the translation of the encoding function encodes the translated function exactly for pure spatial translations, which contains the information relevant for color pattern recognition. In addition, for translations that also have a color component, the error is an

addition of differences between consecutive pixels. This indicates that the encoding is still valid for functions that do not vary very rapidly.

By replacing the expression of the translation, and the definition of $f_E(x,y)$ in equation 23, we obtain the explicit dependence of the two dimensional correlation on the encoded three dimensional functions:

$$C_{2D}[f_E, g_E](Nx'+n', y) = \sum_{x_1=0}^{ND_x-1} \sum_{y_1=0}^{D_y-1} \left[\sum_{n_1=0}^{N-1} \sum_{x_2=0}^{D_x-1} f(x_2, y_1, n_1) \delta_K(x_1 - Nx_2 - n_1) \right] \\ \times \left[\sum_{n_2=0}^{N-1} \sum_{x_3=0}^{D_x-1} g^*(x_3 - x', y_1 - y, n_2 - n') \delta_K(x_1 - Nx_3 - n_2) \right] + E_C(x', y, n') \quad (6.30)$$

Where $E_C(x', y, n')$ is the error in the encoding of the three dimensional correlation. This term comes from the propagation of $E(x', y, n')$. Taking into account that the series indices are independent, and applying the properties of the Kronecker delta function, we can obtain the following expression

$$C_{2D}[f_E, g_E](Nx'+n', y) = \sum_{y_1=0}^{D_y-1} \sum_{n_1=0}^{N-1} \sum_{x_2=0}^{D_x-1} f(x_2, y_1, n_1) g^*(x_2 - x', y_1 - y, n_1 - n') + E_C(x', y, n') \quad (6.31)$$

which is the explicit expression of the three dimensional correlation of $f(x,y,n)$ and $g(x,y,n)$.

$$C_{2D}[f_E, g_E](Nx'+n', y) = C_{3D}[f, g](x', y, n') + E_C(x', y, n') \quad (6.32)$$

Because the translation of the three dimensional function is encoded exactly for translations along the spatial dimensions, $E_c(x',y,n')$ is null for $n'=0$. We have shown in Chapter 5 that the channel of the correlation that must be valued for recognition tasks, is the $n=0$ channel. So, the presented technique can be used for color pattern recognition, because it raises to the exact value of the $n=0$ of the three dimensional correlation.

We give an example in Figure 6.14 to illustrate the encoding technique. The considered scene is the image in Figure 6.14a, and the target object is the top butterfly. The three dimensional function that describes this color image has been encoded onto the image in Figure 6.14b. There, the color dimension has been encoded onto the x -dimension. The result of encoding the x -variable onto the color axis is the image in Figure 6.14c. The magnitude of the $n=0$ channel of the correlation between this scene and the target object obtained by computer simulation, is represented in Figure 6.14d. Figure 6.14e and f, also represent the $n=0$ channel of the correlation, but in this case they have been obtained by using the encoding images in Figure 6.14b and c respectively, and by performing their two dimensional correlations with the target object, which has also been encoded. The scale of the scenes and the correlation profiles are not the same because of the different encoding technique.

One can observe that the magnitude of the $n=0$ channel of the correlation, represented in Figure 6.14d, e and f is the same in the three cases, except by a dilatation of the x axis related to the

decoding of the three dimensional correlation. This shows the suitability of the proposed encoding technique to perform three dimensional correlation. In the three cases, the target object and the non-target object are detected by peaks of similar height, what is expected because both objects have the same shape, and they only differ in their color distributions, which are non saturated colors.

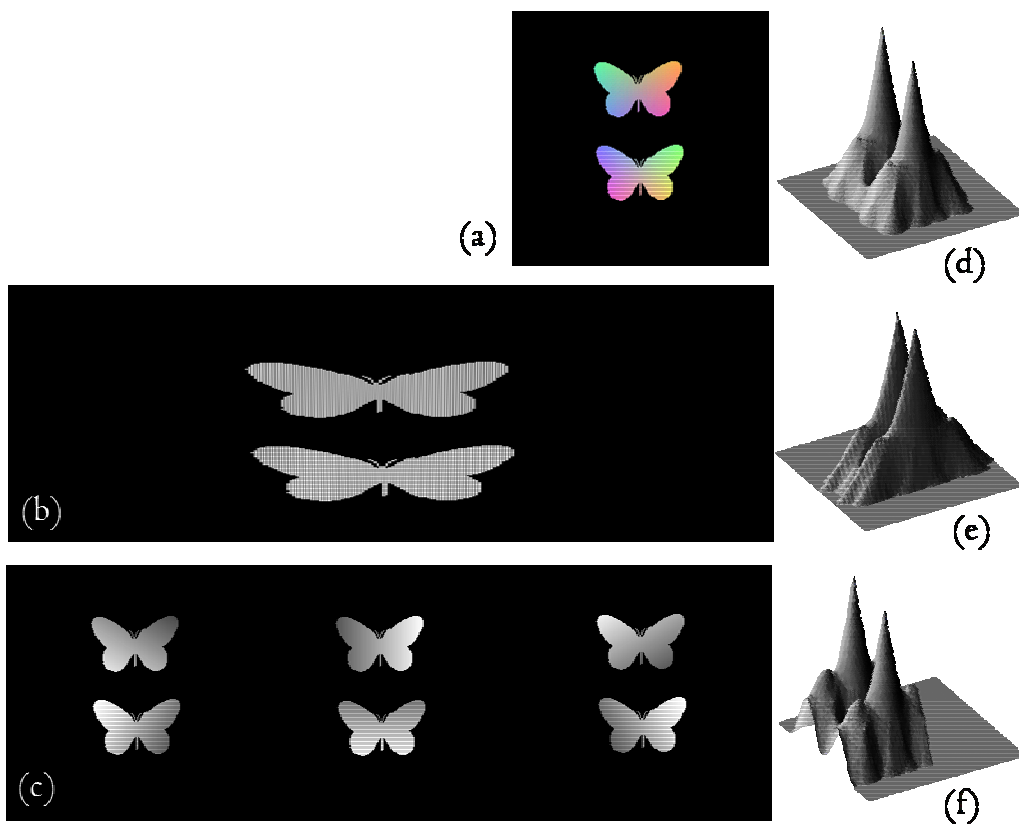


Figure 6.14. Example of the encoding of the three dimensional correlation. (a) color scene. (b) color-encoded Scene (c)spatial-encoded scene (d, e, and f) Magnitude of the $n=0$ channel of the correlation obtained from a, b, and c respectively.

Nevertheless, the encoding technique allows to implement nonlinear filtering to improve the discrimination. We show this in Figure 6.15. The same image in Figure 6.14 has been

considered. The whitening of the color frequency spectrum of the scene leads to the image in Figure 6.15a. We have considered the three dimensional correlation with a phase only filter, which corresponds to the three dimensional whitening of the target object spectrum. This filter is obtained by considering only the phase distribution of the two dimensional Fourier spectrum of the encoding image. We represent the magnitude at the $n=0$ channel of the resulting correlation in Figure 6.15d. Now, the target object is detected by a sharp peak much higher than the non-target object.

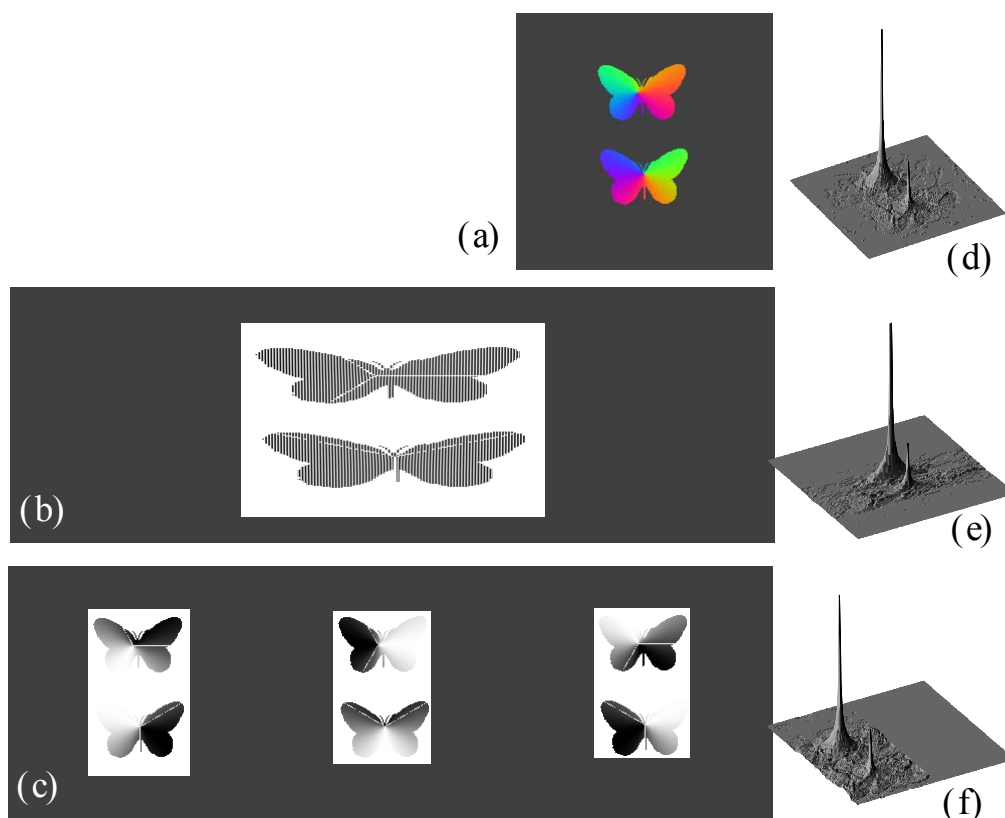


Figure 6.15. Nonlinear correlation. (a) preprocessed color scene. (b) color-encoded scene (c)spatial-encoded scene (d, e, and f) Magnitude of the $n=0$ channel of the correlation obtained from a, b, and c respectively.

The encoding of the correlation leads to the same result. We represent the encoding function for the scene in Figure 6.15b and c. In Figure 6.15b the color is encoded onto the x -dimension and in Figure 6.15d the x -dimension is encoded in the color distribution. The correlation, using a phase only filter, of these scenes with the target object (also encoded) has been represented in Figure 6.15e and f respectively. In both cases the same correlation peaks as for the three dimensional functions are observed. and therefore the target object is clearly discriminated from the non-target one.

6.7.Optical implementation of the three dimensional correlation

The encoding technique presented here has been demonstrated to be useful to perform the three dimensional correlation by means of two dimensional transformations. To implement the technique in an optical correlator, additional aspects have to be taken into account: they can be grouped in two general matters. The quality of the transmission of the channels along the optical system, and the technique used to extract the three dimensional information from the encoding two dimensional image.

We consider two factors that affect the quality of the transmission of the carrier gratings along the correlator. The limitation in the aperture of the elements of the optical system, and the aberrations introduced by these elements. The aberrations introduced by the elements of the optical system

can be compensated by adding the opposite phase to the function represented in the filter SLM. When this is done, the main limitation for the quality of the transmission of the three dimensional information through the correlator is originated by the finite aperture of the elements, that determine the spatial bandwidth of the correlator.

Aside from frequency cuts produced by apertures smaller than the SLMs, and once the scale of the diffraction pattern obtained on the filter is matched to the filter size, the bandwidth of the correlator is determined by the resolution of the SLMs. The maximum frequency that can be represented in the scene SLM corresponds to the grating with a period of two pixels. This is the Nyquist frequency of the system. The scale of the filter is matched so as that the Nyquist frequency of the input SLM is the highest frequency transmitted by the aperture of the filter. The information of the different channels of the image is carried by gratings with period equal to the number N of encoded channels. Therefore, the frequency of the carriers is $2/N$ times the Nyquist frequency of the scene SLM. Therefore, only a certain number of harmonic orders of the carrier gratings will be transmitted by the aperture of the filter. The number of transmitted harmonics n_{MAX} is determined by the number of encoded channels N as follows:

$$n_{MAX} = \begin{cases} \frac{N}{2} & \text{if } N = 2k \text{ (even)} \\ \frac{N-1}{2} & \text{if } N = 2k+1 \text{ (odd)} \end{cases} \quad (6.33)$$

The harmonic removal produces a distortion in the image of the carrier gratings that is formed in the correlation plane. This distortion involves that the image of the pixels of each grating becomes wider than the original image, and consequently it involves the overlapping of the carriers for the different channels. We have represented this situation in Figure 6.16. There, we have considered the encoding gratings for the three channels of an *RGB* color image. We have colored each grating in the color corresponding to the channel it carries, and we have represented the profile and a detail of the reconstructed image of the gratings, for different bandwidth limits. Moreover, we have represented the colors of the resulting image of the gratings on a *B/Y-G/Y* diagram, and we have obtained the clouds of points in the rightmost column of Figure 6.16. This gives a measure of the crosstalk between the channels of the three dimensional function. Figure 6.16a, represents the case where only the fundamental frequency of the grating is transmitted. In this case, the three gratings are mixed each other. Therefore the colors of the gratings are distributed along a curve among the primary colors. When more harmonics are transmitted (Figure 6.16b to d), the peaks of the edges of the squared gratings become sharper and the channels crosstalk becomes small. The fringes of the image of the gratings become more definite and the colors of the image are accumulated near the primary colors. Finally, when the entire series of harmonics is considered, the gratings are perfect square gratings and the only colors in the histogram are the primary colors.

Sometimes the resolution requirements of the input scene are smaller than the resolution of the correlator SLMs. In this case, one can use carrier gratings of period $2N$, $3N$, ...etc. This way, more harmonic orders of the carriers can be transmitted and a better reproduction of the correlation is obtained. We refer to this as half-bandwidth color encoding when the period of the carrier gratings is $2N$.

The other important aspect to consider in the optical implementation of the encoding technique is the acquisition and post-processing of the two dimensional image to decode the three dimensional signal. In particular, one has to take into account that the CCD camera acquires a sample of the image formed in the correlation plane. The sampling frequency is given by the inverse of the distance between the pixels of the camera. In addition, each channel of the three dimensional signal is sampled by a carrier grating. Therefore, it is necessary to adjust the orientation and the period of these samplings so as to establish a correspondence between the pixels of the camera and the image of the pixels of the input scene. So, the channels of the three dimensional correlation are encoded in the columns of the image acquired by the CCD camera.

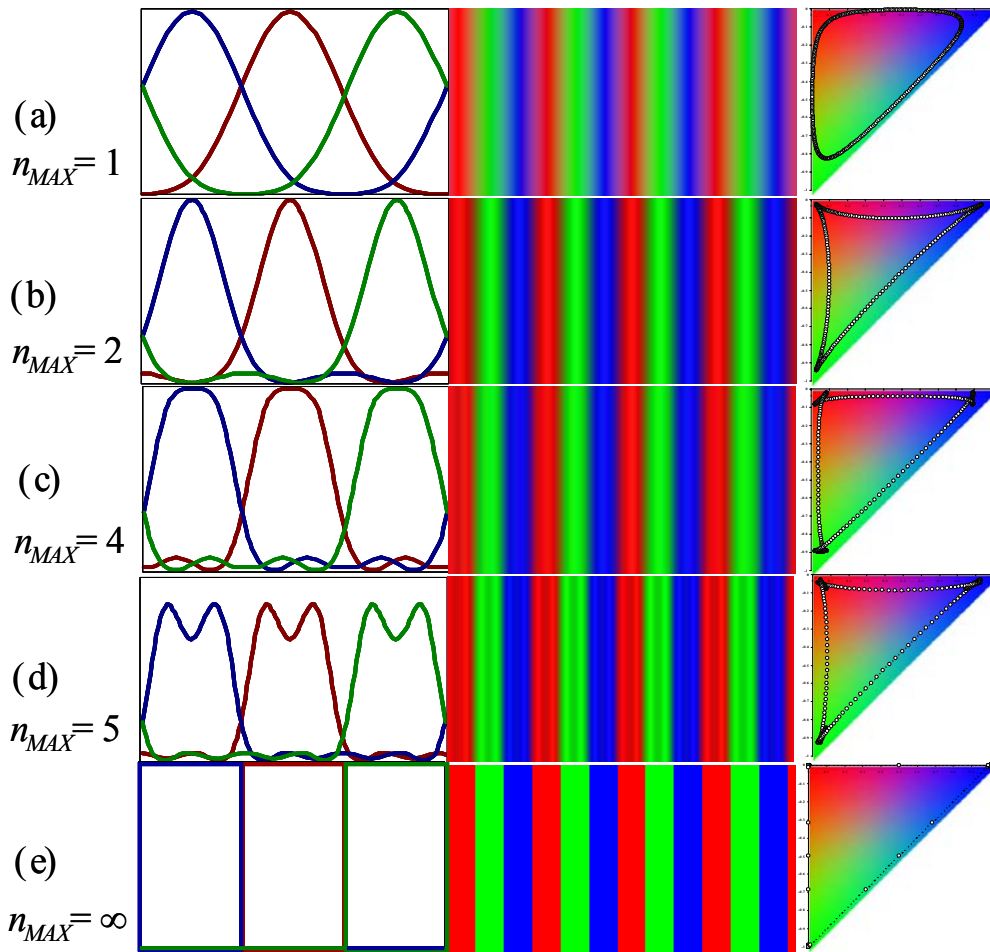


Figure 6.16. Transmission of the carrier gratings corresponding to RGB images by a limited bandwidth correlator. We represent, from left to right, the profile of the shifted gratings, a magnified image of the gratings, and the cloud of points on a B/Y,G/Y diagram.(a) $n_{MAX}=1$, (b) $n_{MAX}=2$, (c) $n_{MAX}=4$, (d) $n_{MAX}=5$, (e) perfect reconstruction of the image of the carriers.

This way, the post-processing of the correlation plane consists of forming the n -th channel of the three dimensional signal in the correlation plane by taking the n -th column of each group of N columns of the acquired image. The post-processing is implemented on the acquisition software developed for the experiment. Because it is a very simple algorithm, it can be

written to be fast enough to obtain the decoded image in real time.

When the encoded signal has three channels a pseudo-colored image can be obtained by assigning each channel of the three dimensional function to one of the primary colors of the *RGB* color scheme. This way, the channel $n=0$ can be colored in red, and the channels $n=1$ and $n=2$ can be colored in green and blue respectively.

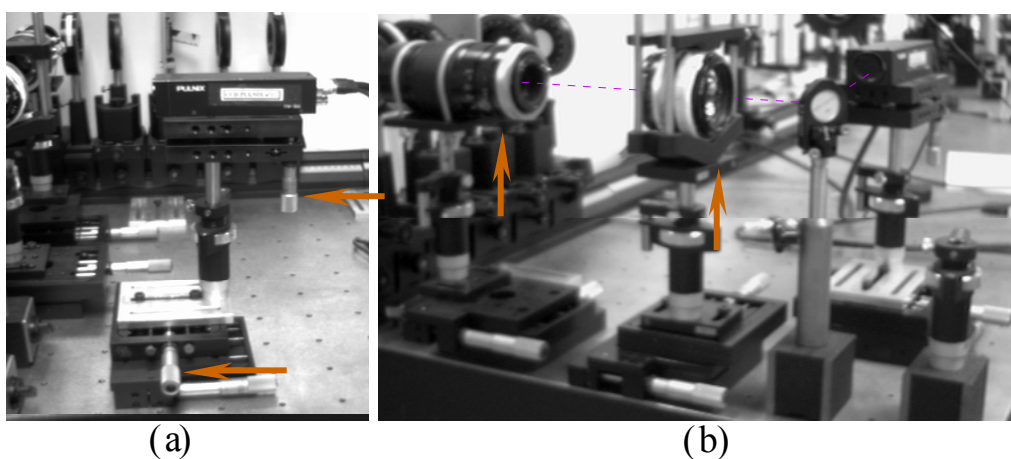


Figure 6.17. (a) Picture of the camera and the twist control mount standing on a lateral shift platform. (b) Picture of the two photographic objectives that compose the zoom system used to control the scale of the correlation on the CCD camera.

To be able to perform the scaling and the alignment of the correlation plane with the CCD pixels, the camera has been based on a mount with precision twist control, and lateral shift control (see Figure 6.17a). Moreover a zoom system composed of two photographic objectives has been used to control the size of the correlation formed in the CCD plane (Figure 6.17b).

To control the alignment between the gratings and the camera we take profit of the Moiré pattern produced by the sampling that the CCD performs on the image of the carrier gratings. The procedure consists of displaying in the input SLM the carrier grating corresponding to one of the channels, keeping uniform the filter SLM, This way, the image of the grating is formed in the correlation plane (Figure 6.18a). This image is acquired by the camera and post-processed in real time by the acquisition software, that displays the color image resulting from the post-processing of the acquired black and white image. This color image is, in general, a fringe pattern like the one shown in Figure 6.18b.

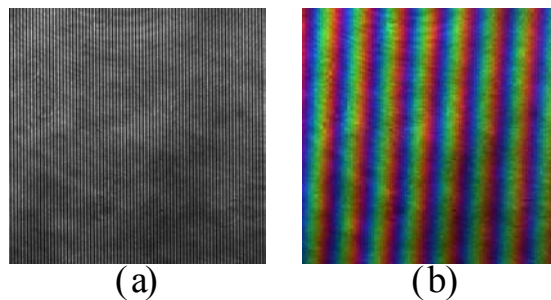


Figure 6.18.(a) image acquired by the CCD camera. (b)Post-processed image.

The width of the gratings is related to the ratio of the frequency of the carrier grating to the sampling frequency of the camera. The fringes become wider when the ratio between these frequencies approaches an integer number, and they disappear when the sampling frequency of the camera is an integer multiple of the frequency of the carrier gratings. The orientation of the fringes is caused by the misalignment of the CCD, and

consequently it can be used to control this misalignment. Therefore, the alignment of the correlation image and the camera can be performed by adjusting the twist control of the camera mount until vertical fringes are observed and by changing the magnification of the zoom until the fringes become infinitely wide. A series of pictures acquired during the alignment process are shown in Figure 6.19. The oblique fringes in Figure 6.19a and b indicate the difference in the orientation between the camera pixels and the input SLM. However, they are more vertical and wide in Figure 6.19b, what indicates that the misalignment is smaller. In Figure 6.19c the only visible fringe is vertical, what indicates that the orientation is the correct one. In addition it is very wide, and this is because the magnification is close to the optimal one. Finally, in Figure 6.19d there are no fringes because in this case the magnification is almost matched, and almost a uniform color is observed.

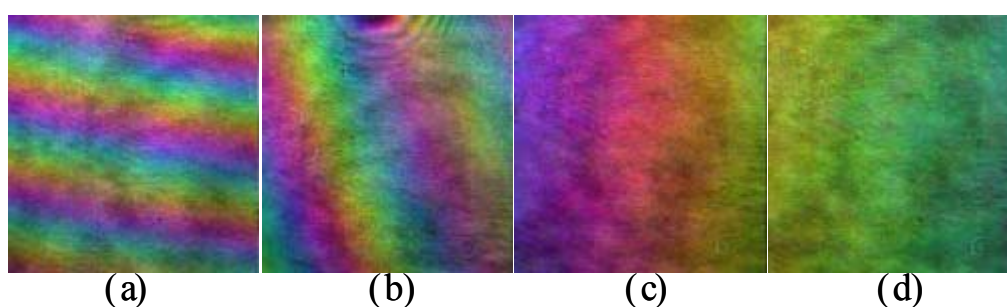


Figure 6.19. Series of post-processed images acquired during the camera alignment procedure. (a) Severe orientation and scale misalignment. (b) Small misalignment. (c) Small scale misalignment, with correct axis orientation (d) Scale and orientation match.

6.8.Experimental results

Once the correlator is properly aligned, and the decoding software is in working order, it can be used to obtain three dimensional optical correlation.

We present the obtained results for three different situations: Full bandwidth color encoding, half-bandwidth color encoding, and spatial encoding. We have considered the color scene in Figure 6.20a, in *RGB* components. The upper butterfly has been used as the target object. So, a three dimensional phase only filter has been matched to it. To generate the three dimensional phase only filter we encode the reference image, in which the target object is represented. Because the two dimensional spectrum of the encoding image encodes the three dimensional spectrum of the encoded image, to whiten the spectrum of the encoded image is equivalent to whiten the three dimensional spectrum, or in other words, to generate a three dimensional phase only filter.

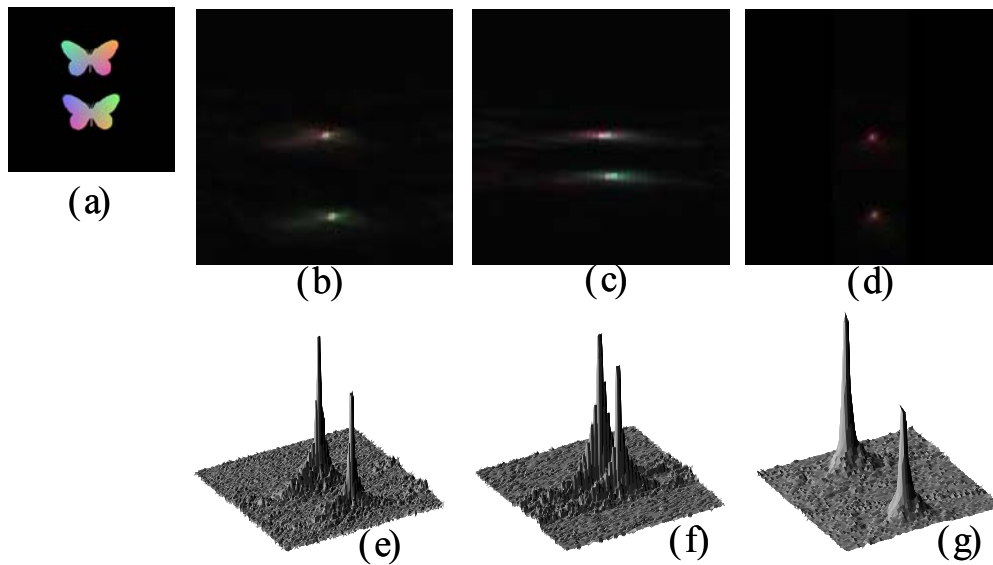


Figure 6.20. Optical implementation of the three dimensional correlation using a phase only filter. (a) Input scene. (b) Full bandwidth color-encoded correlation. (c) Half bandwidth Color-encoded correlation. (d) Spatial encoded correlation. (e) Intensity for (b) at the $n=0$ channel. (f) intensity for (c) at the $n=0$ channel. (g) intensity for (d) at $n=0$.

The experimentally obtained three dimensional correlation has been represented in Figure 6.20b, c and d, for the three mentioned encoding cases. There, the $n=0$ channel is colored in red, and the $n=1$ and $n=2$ are colored in green and blue respectively. Because the two objects have the same shape, in the three cases both objects are detected by a sharp peak. However, one can observe that the color of the peaks is not the same for the two objects, what indicates that the distribution of the peaks in the color axis is not the same. The peak corresponding to the target object is a reddish peak, because its maximum is on the $n=0$ channel, which is colored in red. Meanwhile, the other object peak is greenish, that means that

its maximum is located on the $n=1$ channel, because this is the channel colored in green.

The discrimination of the objects is clearly shown in Figure 6.20e, f and g. There, the intensity at the $n=0$ channel of the correlation for the three encoding cases is represented. In the three cases the peak corresponding to the target object is higher than the other peak. However, because the two objects have the same shape and the colors are very unsaturated colors the discrimination is not very good.

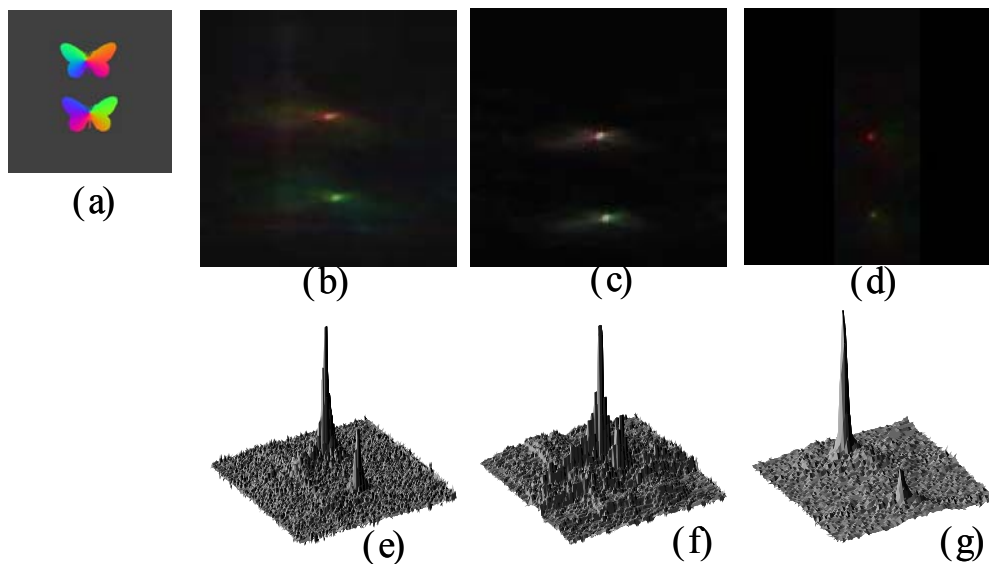


Figure 6.21. Optical implementation of the three dimensional correlation with phase only filter. (a) Preprocessed input scene. (b) Full-bandwidth color-encoded correlation. (c) Half bandwidth color-encoded correlation. (d) Spatial encoded correlation. (e) Intensity for (b) at the $n=0$ channel. (f) Intensity for (c) at the $n=0$ channel. (g) Intensity for (d) at $n=0$.

As we explained in Chapter 4 the three dimensional auto-correlation presents its maximum in the $n=0$ channel, independently of the color distribution of the target. Because we

assign the $n=0$ channel to the red component of the color image of the correlation, the peak corresponding to the target object appears colored in red.

The discrimination of the correlation can be improved by a simple preprocessing of the input scene (See Section 5.8). We have done this for the studied scene. The preprocessed scene is represented in Figure 6.21a. There the colors of the butterflies are saturated colors, and a constant has been added to the whole scene to avoid the negative values, and to allow its representation in a SLM. As the scene is also represented by a three dimensional function it can be encoded by the proposed techniques. So, we have obtained the three dimensional correlation of this scene, using a phase only filter matched to the upper butterfly. We remark that the filter is the same filter we have used for the results presented in Figure 6.20, because it was the result of whitening the three dimensional spectrum of the target object. The pseudo-colored image that represents the correlation for the cases of Full bandwidth color-encoding, half bandwidth color-encoding, and spatial encoding is presented in Figure 6.21b, c and d respectively. The intensity at the $n=0$ channel for the three cases is presented in Figure 6.21e, f and g. Again, the two objects are detected by sharp peaks with different colors, being red the peak corresponding to the target object, (the $n=0$ channel is colored in red) and green the peak corresponding to the other object (corresponding to the $n=1$ channel). However in this case, for the three variants of the

encoding technique, the colors of the peaks are more saturated than for the scene in *RGB* coordinates in Figure 6.20: In other words, the peaks are also sharper along the color axis. Therefore, at the $n=0$ channel of the three dimensional correlation(Figure 6.21e, f and g) the peak corresponding to the non target object is now very small in comparison to the autocorrelation peak, what indicates that the discrimination is improved, and correctly encoded by the three variants of the proposed technique.

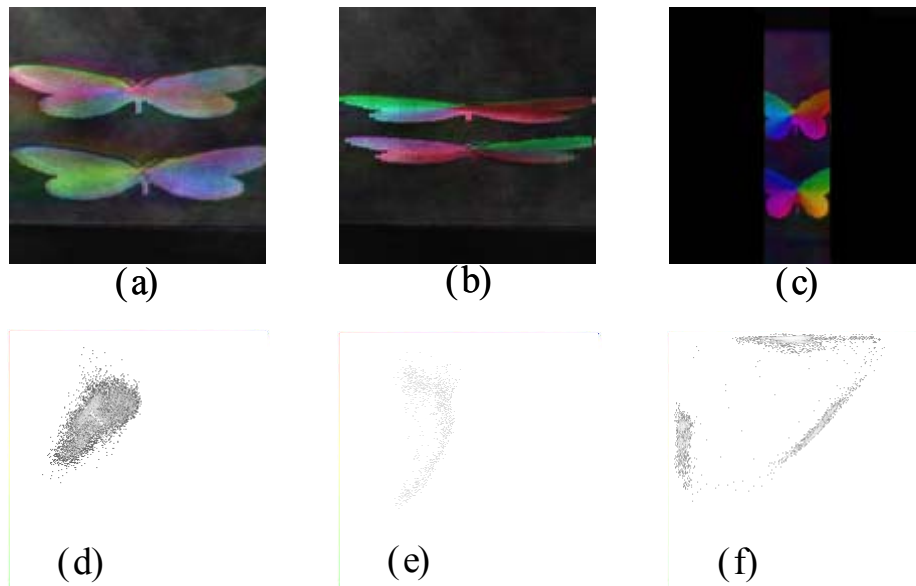


Figure 6.22. Image of the preprocessed scene through the correlator and the decoding software. (a) Full bandwidth color-encoding. (b) Half bandwidth color encoding. (c) Spatial encoding. (d),(e) and (f) Histograms on the plane $B/Y-G/Y$ of (a),(b) and (c) respectively.

One can observe that the discrimination is improved in the three encoding cases: However, the ratio of the peaks is not the same for the three cases. This is because the bandwidth limit of the optical correlator affects in different way the different

encoding. To illustrate this we have represented in Figure 6.22 the image of the preprocessed scene obtained at the correlation plane when a uniform filter is used in the correlator, for the three encoding cases. The images shown in Figure 6.22a b and c correspond to the color images obtained after the acquisition and the post-processing of the encoded scenes Figure 6.22d, e and f are their corresponding histograms on the $B/Y-G/Y$ plane.

We can observe that in the case of the Full bandwidth color-encoding (Figure 6.22a and d), the colors in the image of the scene are quite unsaturated colors because in this case only the DC term and the fundamental orders of the carrier gratings are transmitted, and therefore the channels are mixed, generating unsaturated colors. In the case of Half bandwidth color-encoding, the second and third harmonic orders of the carrier gratings are also transmitted, and therefore their reconstruction is better, as can be seen in Figure 6.22b. Therefore, the colors of the post-processed image are more saturated than in Figure 6.22a, as the corresponding histogram indicates(Figure 6.22e). Finally, we observe the case of the spatial encoding. Because we consider a 100 pixels width image, 50 harmonic orders are transmitted through the correlator. In this case, the carrier gratings are very well transmitted and the scene is very well reproduced (Figure 6.22c) and the colors (of the preprocessed scene) are saturated, as can be seen in Figure 6.22f. This gives the best discrimination as can be seen in Figure 6.21g.